

Design of flat-band superprism structures for on-chip spectroscopy

Boshen Gao,¹ Zhimin Shi^{2,*} and Robert W. Boyd^{1,3}

¹The Institute of Optics, University of Rochester, Rochester, New York 14627, USA

²Department of Physics, University of South Florida, Tampa, Florida 33620, USA

³Department of Physics and School of Electrical Engineering and Computer Science, University of Ottawa, Ottawa, K1N 6N5, Canada

[*zhiminshi@usf.edu](mailto:zhiminshi@usf.edu)

Abstract: We present a systematic design procedure of photonic crystal (PhC) superprism structures for on-chip spectroscopic applications. In specific, we propose a new figure of merit, namely the angular-group-dispersion-bandwidth-product (AGDBP) to quantitatively describe the spectroscopic performance of PhC superprism structures, and an optimum PhC structure for spectroscopic applications should have large angular group dispersion over a large bandwidth, i.e., a flat-top dispersion profile. We demonstrate the advantage of such a new design consideration by optimizing the geometry of a two-dimensional parallelogram-lattice PhC superprism structure. The performance of such a superprism spectrometer is further analyzed numerically using finite-difference time-domain simulations, which out-performs current implementations in terms of the number of achievable output spectral channels.

© 2015 Optical Society of America

OCIS codes: (050.5298) Photonic crystals; (120.6200) Spectrometers and spectroscopic instrumentation; (130.7408) Wavelength filtering devices; (130.3120) Integrated optics devices.

References and links

1. E. Yablonovitch, "Inhibited spontaneous emission in solid-state physics and electronics," *Phys. Rev. Lett.* **58**, 2059–2062 (1987).
2. S. John, "Strong localization of photons in certain disordered dielectric superlattices," *Phys. Rev. Lett.* **58**, 2486–2489 (1987).
3. J. D. Joannopoulos, P. R. Villeneuve, and S. Fan, "Photonic crystals: putting a new twist on light," *Nature* **386**, 143–149 (1997).
4. R. A. Shelby, D. R. Smith, and S. Schultz, "Experimental verification of a negative index of refraction," *Science* **292**, 77–79 (2001).
5. J. Witzens, M. Loncar, and A. Scherer, "Self-collimation in planar photonic crystals," *IEEE J. Sel. Top. Quantum Electron.* **8**, 1246–1257 (2002).
6. S.-Y. Lin, V. M. Hietala, L. Wang, and E. D. Jones, "Highly dispersive photonic band-gap prism," *Opt. Lett.* **21**, 1771–1773 (1996).
7. H. Kosaka, T. Kawashima, A. Tomita, M. Notomi, T. Tamamura, T. Sato, and S. Kawakami, "Superprism phenomena in photonic crystals," *Phys. Rev. B* **58**, R10096–R10099 (1998).
8. H. Kosaka, T. Kawashima, A. Tomita, M. Notomi, T. Tamamura, T. Sato, and S. Kawakami, "Superprism phenomena in photonic crystals: Toward microscale lightwave circuits," *J. Lightwave Technol.* **17**, 2032 (1999).
9. T. Baba and M. Nakamura, "Photonic crystal light deflection devices using the superprism effect," *IEEE J. Quantum Electron.* **38**, 909–914 (2002).
10. B. Momeni and A. Adibi, "Systematic design of superprism-based photonic crystal demultiplexers," *IEEE J. Sel. Areas Commun.* **23**, 1355–1364 (2005).
11. B. Momeni, J. Huang, M. Soltani, M. Askari, S. Mohammadi, M. Rakhshandehroo, and A. Adibi, "Compact wavelength demultiplexing using focusing negative index photonic crystal superprisms," *Opt. Express* **14**, 2413–2422 (2006).

12. B. E. Nelson, M. Gerken, D. A. B. Miller, R. Piestun, C.-C. Lin, and J. S. Harris, "Use of a dielectric stack as a one-dimensional photonic crystal for wavelength demultiplexing by beam shifting," *Opt. Lett.* **25**, 1502–1504 (2000).
13. D. Bernier, X. L. Roux, A. Lupu, D. Marris-Morini, L. Vivien, and E. Cassan, "Compact, low cross-talk cwdm demultiplexer using photonic crystal superprism," *Opt. Express* **16**, 17209–17214 (2008).
14. S. G. Johnson and J. D. Joannopoulos, "Block-iterative frequency-domain methods for maxwell's equations in a planewave basis," *Opt. Express* **8**, 173–190 (2001).
15. T. Baba and T. Matsumoto, "Resolution of photonic crystal superprism," *Appl. Phys. Lett.* **81**, 2325–2327 (2002).
16. A. F. Oskooi, D. Roundy, M. Ibanescu, P. Bermel, J. D. Joannopoulos, and S. G. Johnson, "MEEP: A flexible free-software package for electromagnetic simulations by the FDTD method," *Comput. Phys. Commun.* **181**, 687–702 (2010).
17. B. Momeni and A. Adibi, "An approximate effective index model for efficient analysis and control of beam propagation effects in photonic crystals," *J. Lightwave Technol.* **23**, 1522 (2005).
18. J. Witzens, T. Baehr-Jones, and A. Scherer, "Hybrid superprism with low insertion losses and suppressed cross-talk," *Phys. Rev. E* **71**, 026604 (2005).
19. B. Momeni and A. Adibi, "Adiabatic matching stage for coupling of light to extended bloch modes of photonic crystals," *Appl. Phys. Lett.* **87**, 171104 (2005).
20. D. Bernier, E. Cassan, X. Le Roux, D. Marris-Morini, and L. Vivien, "Efficient band-edge light injection in two-dimensional planar photonic crystals using a gradual interface," *Opt. Eng.* **48**, 070501 (2009).

Introduction

Photonic crystals (PhCs) [1–3] are periodic dielectric patterns with feature sizes comparable to the wavelength of light. Such a strong modulation of the dielectric constant within the medium results in banded features much like what a real crystal does to an electron. Moreover, the dispersion relation of light can differ significantly from that of a homogeneous medium especially near the photonic band edge. Such an effect can lead to many unconventional optical properties, e.g., negative refraction [4], self-collimation [5], superprism effects [6–9], etc.

The term "superprism" refers to the effect that light beams with slightly different frequencies propagate in very different directions within the PhC region. Such a strong angular dispersion is promising for constructing compact on-chip demultiplexers for spectroscopic or wavelength-division-multiplexing communication applications [10–13].

Many previous studies of the superprism effect concentrated primarily on achieving an angular group dispersion (AGD) as large as possible. However, large AGD typically occurs only over a very narrow range of frequencies, and is highly frequency dependent. Using such a superprism structure to construct a spectrometer would lead to highly nonuniform channel spacing over a narrow working bandwidth. On the contrary, an ideal spectrometer would possess uniform spectral resolution over a large working bandwidth, i.e., would possess a flat-top dispersion profile. To incorporate such an idea into the design of a superprism structure, we here propose a new figure of merit (FOM), namely the angular-group-dispersion-bandwidth product (AGDBP) to quantitatively describe the spectroscopic performance of PhC superprism structures. Using this new metric, we perform an optimization of the geometry of a two-dimensional parallelogram-lattice PhC structure to achieve flat-band operation. The spectral performance of one example of a superprism-based on-chip spectrometer is further analyzed numerically using finite-difference time-domain simulations.

Analysis of PhC superprism structures

We first briefly summarize the mathematical formula used to quantitatively describe the angular dispersion performance of a given superprism PhC structure. We start with a 2-D square-lattice PhC structure as shown in the inset of Fig. 1, where \mathbf{a}_1 and \mathbf{a}_2 are the basis vectors and r is the radius of each air hole drilled into the host material. We use a plane wave expansion analysis algorithm [14] to calculate the bandstructure of such a PhC, and the calculated equi-frequency contours (EFC) in the first Brillouin zone are plotted in Fig. 1.

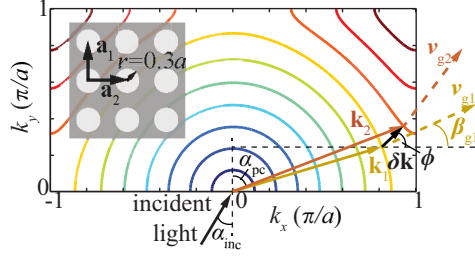


Fig. 1. Equi-frequency contours (EFCs) of a 2-D square lattice PhC in the first Brillouin zone. The light beam enters the PhC region at an incidence angle α_{inc} and the “refraction” angle inside the PhC region is labeled as α_{pc} . Solid arrows are the Bloch \mathbf{k} vectors indicating the direction of phase velocities of the beams. Dashed arrows normal to the EFC contour indicates the directions of group velocities. Near the band edge in k -space, a small change in frequency leads to a large directional variation in group velocity. Inset: the PhC structure in real space. \mathbf{a}_1 and \mathbf{a}_2 are the two basis vectors. The radius of the air holes is $r = 0.3a$ where $a = |\mathbf{a}_1|$ is the lattice constant.

We assume that the interface between the PhC and the incident slab medium is along one lattice direction, denoted by \mathbf{a}_1 . To quantify the superprim effect, we define the angular group dispersion (AGD), also sometimes referred to as the q factor [15] at a frequency ω as follows:

$$q(\alpha_{\text{inc}}, \omega) = \left. \frac{\partial \beta_g}{\partial \omega} \right|_{\alpha_{\text{inc}}}, \quad (1)$$

where α_{inc} is the incidence angle from a slab medium with an effective refractive index n_{slab} , and where β_g denotes the angle between the group velocity vector and the k_x axis. The value of β_g can be obtained using the following equation:

$$\tan \beta_g = \frac{\partial \omega / \partial k_y}{\partial \omega / \partial k_x}. \quad (2)$$

Since one can obtain the numerical values of the partial derivatives $\partial \omega / \partial k_x$ and $\partial \omega / \partial k_y$ by analyzing the calculated band structure, expression (1) can be rewritten as follows:

$$q = \frac{\partial \beta_g / \partial \mathbf{k} |_{\alpha_{\text{inc}}}}{\partial \omega / \partial \mathbf{k} |_{\alpha_{\text{inc}}}}. \quad (3)$$

For light incident from a fixed direction, a frequency change $\delta \omega$ leads to a change in the Bloch wave vector \mathbf{k} inside the PhC as follows:

$$\delta \mathbf{k} = \frac{\delta \omega}{d\omega/dk_\phi} \hat{\mathbf{u}}_\phi, \quad (4)$$

where $\hat{\mathbf{u}}_\phi$ is the unit vector along $\delta \mathbf{k}$ and ϕ is the angle between this vector and the k_x axis. Employing the boundary conditions at the interface and solving for ϕ , we have

$$\tan \phi = \left(\frac{\omega}{|k| \sin \alpha_{\text{phc}}} - \frac{\partial \omega}{\partial k_x} \right) / \frac{\partial \omega}{\partial k_y}, \quad (5)$$

where α_{phc} is the effective refraction angle of the incident field within the PhC region. This relation determines the direction of the derivatives in Eq. (2) that should be taken, and the

numerical values of q can eventually be determined using numerically obtainable quantities as follows:

$$q = \frac{\left(\frac{\partial \omega}{\partial k_x} \frac{\partial^2 \omega}{\partial k_x \partial k_y} - \frac{\partial^2 \omega}{\partial k_x^2} \frac{\partial \omega}{\partial k_y} \right) \cos \phi + \left(\frac{\partial \omega}{\partial k_x} \frac{\partial^2 \omega}{\partial k_y^2} - \frac{\partial^2 \omega}{\partial k_x \partial k_y} \frac{\partial \omega}{\partial k_x} \right) \sin \phi}{\left[\frac{\partial \omega}{\partial k_x} \cos \phi + \frac{\partial \omega}{\partial k_y} \sin \phi \right] \left[\left(\frac{\partial \omega}{\partial k_x} \right)^2 + \left(\frac{\partial \omega}{\partial k_y} \right)^2 \right]}. \quad (6)$$

Lattice structure optimization

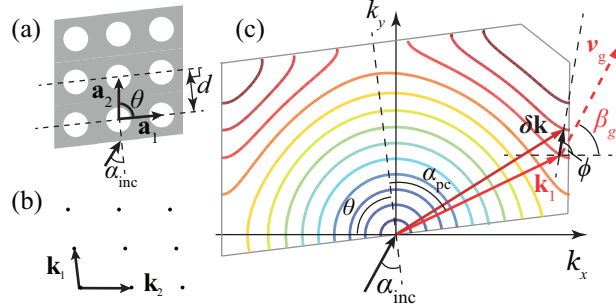


Fig. 2. Geometric analysis of beam propagation in a general 2-D PhC. (a), the PhC structure in coordinate space; θ and d are the two adjustable parameters. (b), corresponding reciprocal lattice; \mathbf{k}_1 is perpendicular to \mathbf{a}_1 and \mathbf{k}_2 to \mathbf{a}_2 . (c), EFC plot of the structure. The k_x axis is chosen to be along the \mathbf{k}_2 direction.

One major limitation of a square-lattice PhC superprism structure is that its AGD is highly frequency dependent, which leads to very narrow working bandwidth over which the superprism effect is appreciable and to very unevenly-spaced channel spacing.

On the other hand, spectroscopic applications typically desire a spectrometer to distinguish many uniformly-distributed spectral lines over the bandwidth of interest. Such concern indicates that an ideal superprism spectrometer should have uniform AGD over an extended working bandwidth. To take into account such considerations, we here propose a new figure of merit, namely the angular-group-dispersion-bandwidth product (AGDBP) defined as follows:

$$\mathcal{P}(\omega_0) = q(\omega_0) \Delta \omega. \quad (7)$$

Here $q(\omega_0)$ is the AGD at a central frequency ω_0 , and $\Delta \omega$ is the frequency bandwidth in the vicinity of ω_0 within which the AGD varies less than 5% from $q(\omega_0)$.

To optimize the PhC structure to achieve better spectral performance, we generalize the square PhC lattice into a parallelogram lattice as shown in Figs. 2(a) and 2(b). A parallelogram lattice can be described using several free parameters: the angle θ between the two basis vectors \mathbf{a}_1 and \mathbf{a}_2 , and the distance d between neighboring rows of air holes, and the radius of air holes r . For illustrative purposes, we here choose to fix r at a typical value $r = 0.3a$ and to optimize only the two parameters θ and d . Note that $|\mathbf{a}_2| \equiv a_2 = d / \cos \theta$.

For a given PhC structure with a set of values for θ and d , we first calculate the value of \mathcal{P} for all possible incidence angle α_{inc} as shown in Fig. 2(a) using the procedure described in the previous section. We then select the maximum value \mathcal{P}_{max} as the optimum AGDBP of the structure with the current set of θ and d . Considering practical fabrication conditions, we here limit the value of d to be between $0.9a_1$ and $1.5a_1$, and the value of θ between 90° and $90^\circ - \tan^{-1}(0.5a_1/d)$. Note that for a given value of d , our scanning range of θ covers

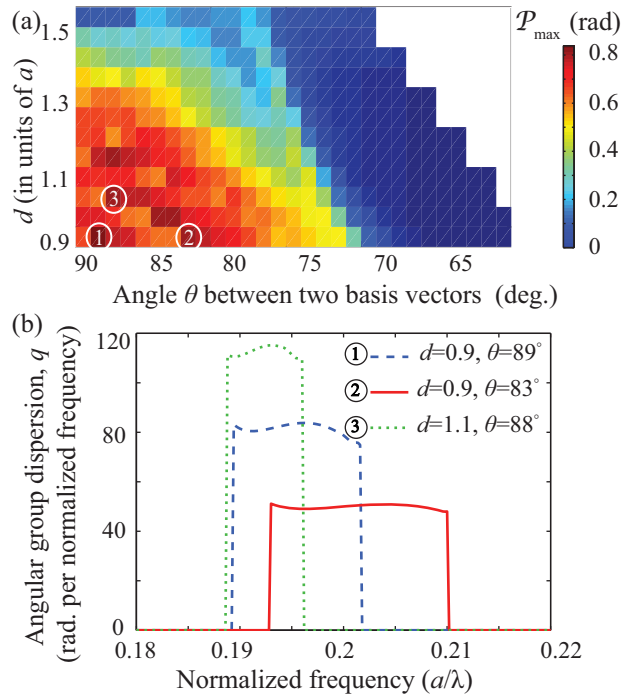


Fig. 3. Optimization results for obtaining a flat-band PhC superprism. (a), \mathcal{P}_{\max} as a function of position in the two dimensional parameter space. (b) Superprism factor q as a function of the normalized frequency ω plotted for 3 structures: ① $\mathcal{P}_{\max} = 0.839$ rad, $d = 0.9a_1$, $\theta = 89^\circ$; ② $\mathcal{P}_{\max} = 0.802$ rad, $d = 0.9a_1$, $\theta = 83^\circ$; ③ $\mathcal{P}_{\max} = 0.809$ rad, $d = 1.1a_1$, $\theta = 88^\circ$.

all possible geometries for all incidence angles due to the symmetry and periodicity of the PhC structures. The optimum AGDBP \mathcal{P}_{\max} is plotted in Fig. 3(a) as a function of θ and d . Here the effective refractive index of the slab is 2.83, and only TE polarization is considered. Figure 3(b) shows the optimized AGD as a function of frequency for three different sets of optimized parameters as circled in Fig. 3(a). All three designs exhibit flat-band AGD over extended frequency ranges, and therefore can satisfy various differing needs for the working bandwidth.

Numerical demonstration of an optimized superprism spectrometer

To further demonstrate the performance of our flat-band PhC superprism structure obtained through the optimization procedure, we numerically simulate spectral performance of an optimized superprism spectrometer using finite-difference time-domain (FDTD) algorithms [16]. The lattice parameter of the PhC structure is chosen to be $d = 0.9a_1$, $\theta = 89^\circ$, i.e., the structure ① marked in Fig. 3(b). We further choose the lattice constant a_1 to be 310 nm, which would set the center wavelength at 1550 nm with a working bandwidth of approximately 80 nm.

The schematic diagram of this spectrometer is shown in Fig. 4(a). The device is composed of an adiabatically tapered input waveguide, a preconditioning free-propagation region (a slab waveguide) [11], a PhC superprism region, a second free-propagation slab region, and a series of single-mode output waveguides corresponding to individual output channels. Light is launched into the structure from the input waveguide. This input waveguide is adiabatically

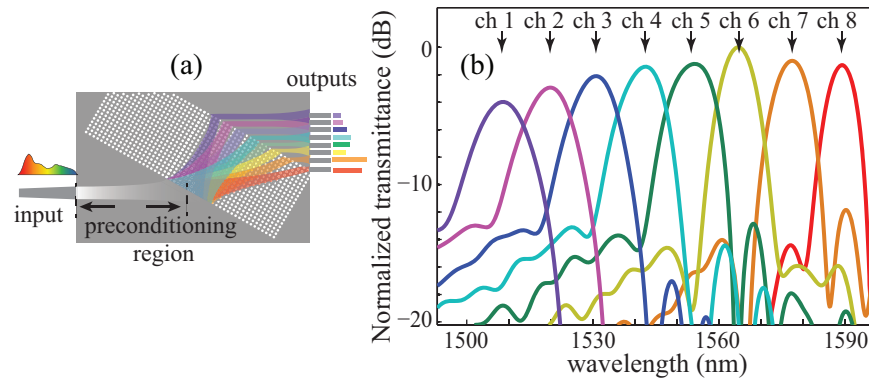


Fig. 4. (a) Schematic diagram of a flat-band superprism spectrometer; (b) Spectral transmission of the 8 channels that are evenly spaced over the working bandwidth.

widened to an exit-width of $3.72\ \mu\text{m}$ in order to reduce the angular spatial frequency components of the input beam. The preconditioning region is designed to be $140\ \mu\text{m}$ long and has opposite sign in the second-order diffraction coefficient [17] as compared to that in the PhC region. As a result, the beam first diverges in the preconditioning region and then re-focuses as it propagates within the PhC region. The total PhC area is approximately $135\ \text{by}\ 42\ \mu\text{m}^2$. The spacing between neighboring output waveguides is approximately $3.5\ \mu\text{m}$. The output signals are coupled into 8 single-mode waveguides. Figure 4(b) shows the normalized spectral transmittance of the 8 channels. As predicted by the design, this device shows a quite flat spectral response over its designed working bandwidth, and the number of channels it can support is approximately doubled as compared to previous designs [10–13]. The peak transmission varies by approximately 4 dB over the eight channels, and the spectral response slightly widens from channel 8 to channel 1. Such non-uniformity in transmission and the crosstalk between the channels are primarily caused by the aberrations, e.g., spherical and coma, of the spectrometer geometry that involves a rectangular PhC region. These aberrations can be potentially reduced by optimizing the shape and local lattice geometries of the PhC region [18]. The on-chip loss of the spectrometer is simulated to be approximated 11–15 dB, which is mainly caused by the undesired reflection at the slab-PhC interfaces. Such reflections can be mitigated by adiabatically optimizing the PhC structures at the vicinity of the slab-PhC interfaces [19, 20].

Conclusion

In this work, we have proposed a new figure of merit, namely the angular-group-dispersion-bandwidth-product to quantify the spectroscopic performance of a PhC superprism structure. Using this FOM, we have performed optimization of a parallelogram-lattice PhC structure for building a superprism spectrometer. We have shown that a flat angular group dispersion can be achieved for a wide range of working bandwidths. Furthermore, the performance of an 8-channel spectrometer with 10 nm channel spacing at the center wavelength of 1550 nm has been determined using numerical simulation. Our method provides a systematic procedure to design flat-band on-chip miniaturized spectrometers and demultiplexers based on photonic crystals, and can be extended straightforwardly to other dispersive mechanisms.

Acknowledgments

The authors thank A. C. Liapis and S. Schultz for helpful discussions, and gratefully acknowledge support by the U.S. Defense Threat Reduction Agency.